6.3

A STATISTICAL APPROACH TO A LAGRANIAN PERSPECTIVE OF CIRRUS EVOLUTION BASED ON DATA FROM THE INCA EXPERIMENTS IN THE NORTHERN AND SOUTHERN HEMISPHERE MIDLATITUDES

J. Ström(1), M. Seifert(1), R. Krejci(1), A. Minikin(2), A. Petzold(2), Gayet J-F(3), F. Auriol(3), J. Ovarlez(4) and U. Schumann(2)

(1) Institute of Applied Environmental Research, Stockholm University, Sweden
(2) Institut für Physik der Atmosphäre, DLR, Oberpfaffenhofen, Germany
(3) Laboratoire de Météorologie Physique, UMR / CNRS n° 6016, Université Blaise Pascal, Clermont-Fd, France
(4) Laboratoire de Météorologie Dynamique, Ecole Polythechnique, Palaiseau, France

Data presented below was collected during two field campaigns in spring and fall of 2000 as part of the EU funded project INCA (Interhemispheric differences in cirrus properties from anthropogenic emissions). The first experiment was conducted in March/April from Punta Arenas, Chile (54S) and the second experiment was conducted in October/November from Prestwick, Scotland (53N).

The analysis will show that by using a very simple phenomenological model and assuming a vertical wind distribution given by a cascade of gravity waves, several statistical features of cirrus clouds can be captured when presenting the data as a function of crystal number density and relative humidity.

Figure 1 below shows the number of observations as a function of the logarithm of the crystal number density and the relative humidity over ice. The crystal number density is measured by the CVI (Counterflow Virtual Impactor) and the humidity is measured using a frostpoint hygrometer. The data is from the Prestwick campaign at an altitude above 6 km and temperatures below 235K.

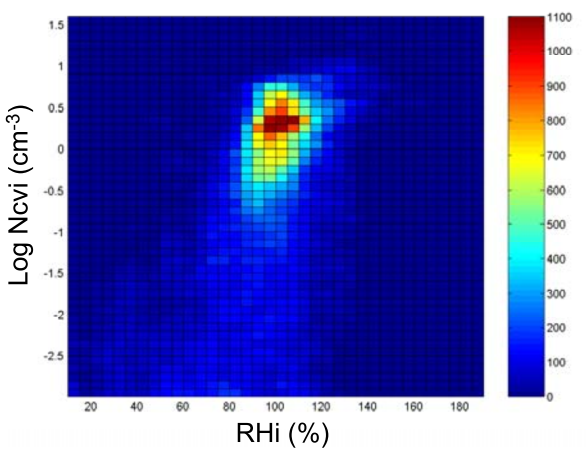

Figure 1. Color-coded frequency distribution of observations as function of relative humidity over ice and crystal number density. Data from the Prestwick campaign at temperatures below 235K. The data is a composite of 9 mission flights.

Corresponding author address: Johan Ström, Inst. of Applied Environmental Research, Stockholm Univeristy, S-106 91 Stockholm, Sweden. E-mail: johan@itm.su.se

The frequency distribution in Figure 1, present a distinct maximum at approximately 100% RHi and 2cm^{-3}. The number of observations decreases quickly around this maximum, but a veil of blue shades is extending down towards lower humiditis and lower crystal number densities.

If the data presented in Figure 1 is normalized to the maximum frequency for each humidiy increment a different pattern appears, which is presented in Figure 2. In this plot the information about the number of observations is lost and each humidity interval have the same weight. If neighboring cells, or combinations of Ncvi and RHi, were uncorrelated a stochastic mosaic would be displayed in Figure 2. Therefore, connecting maximums in the figure indicates preferred pathways for the cloud parameters assuming that the cloud form at high humidities and disappears at low humidities.

Prior to the cloud appear the conditions are below the Ncvi-scale and above 100% RHI. Once the cloud form crystals appear quickly without changing the ambient humidity very much. As the crystals grow they begin to deplete excess water vapor at a rate faster than it is supplied and the humidity is starting to decrease.

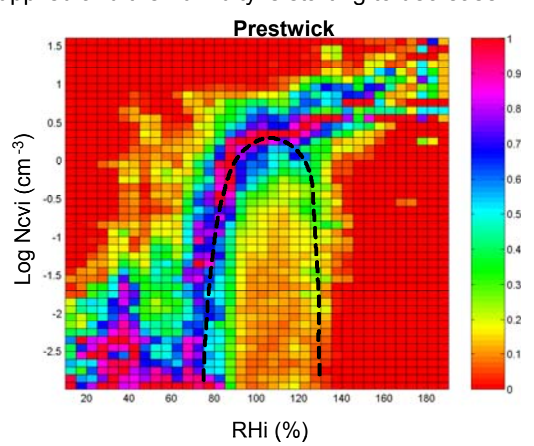

Figure 2. Same data as in Figure 1, but normalized to the maximum frequency at each given humidity. The dashed line indicates a suggested pathway for the evolution of cirrus for an ensample of clouds.

This is where the maximum crystal number density in the parcel is achieved. After this point is reached the crystals in the cloud simply grows until the humidity have relaxed down to 100% RHi. As the ambient humidity drops below 100% RHi, the crystals begin to evaporate and the number density drops quickly with decreasing RHi. This sequence is indicated by the dashed line in Figure 2.

This Lagranian interpretation of the features in Figure 2, which is based on data from nine flights, also suggests that a systematic relation to the driving force (vertical wind) should be present. In average the forming part of the cloud should have positive winds (updrafts), while the dissolving part could be either negative or zero but hardly positive. The average vertical wind plotted in Figure 3 show exactly this. Relative humidity above 100% RHi is associated updrafts whereas relative humidity below 100% RHi is associated with downdrafts

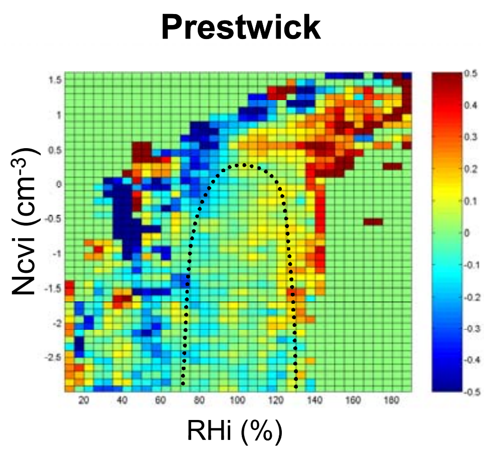

Figure 3. Average vertical for the same data as presented in Figures 1 and 2.

That cirrus clouds form in updraft regions is not a new in sight and has been illustrated very well in case studies, but Figure 3 shows that the relation between vertical wind, relative humidity, and crystal number density is very strong even in a statistical sense.

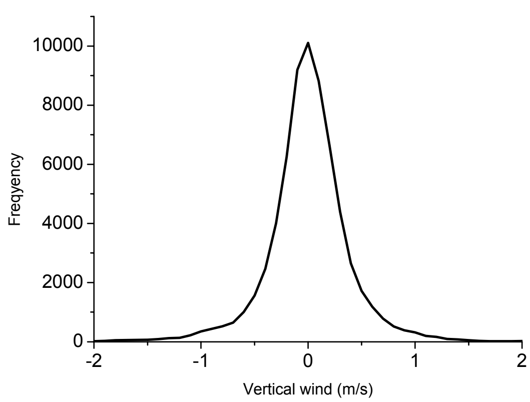

Figure 4. Frequency distribution of vertical wind velocity during the Prestwick campaign.

Would it be possible to reproduce some of the features seen in Figures 1, 2, and 3 by using a simple numerical model that emulate the evolution of cirrus clouds? The first problem is what updraft velocity to use. Most process models (parcel models) use a constant updraft and terminate the simulation after some given time. Figure 4 shows the frequency distribution of vertical wind during the Prestwick campaign (the distribution for Punta Arenas is almost identical). The most typical vertical wind in Figure 4 is 0 m/s, with a rapidly decreasing probability towards larger amplitudes. Hence, using the most typical wind will not work.

We may pick any wind larger than zero, but we still do not know the evolution of the wind for a particular air parcel. We note that if the dashed line in Figure 2 is projected in Figure 3 the average vertical winds along this line presents something that resembles a wave according to the color scale in Figure 3. This observation opens some possibilities.

We postulate that cirrus formation is always associated with wave motions and that large-scale uplifts are of second order importance since even small wave perturbations may be significantly larger than synoptic scale motions. A wave can be described as in eq. 1.,

$$w(t) = amp \sin\left(\pi \frac{t}{T}\right) \quad (1)$$

where the vertical wind at a given time is given by the maximum amplitude and a characteristic period T. However, a wave does not have the same distribution of vertical winds as in Figure 4. In order to reproduce the observed distribution of vertical winds we need to have a cascade of waves of different scales or maximum amplitudes. If the probability for a wave with a given maximum amplitude (amp) is given by,

$$P(amp)\alpha \frac{1}{10^{amp}} \quad (2)$$

the observations can be reproduced very well.

Figure 5 show the distribution resulting from the combination of eq. 1 and eq. 2, together with the observed distribution.

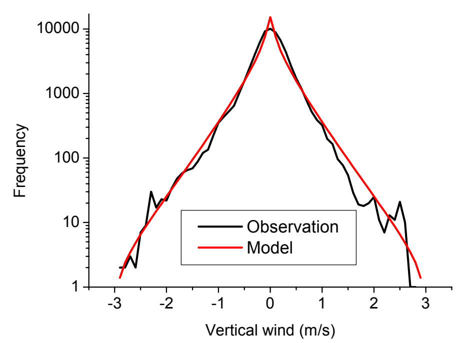

Figure 5. Frequency distribution of vertical wind velocities (black line) as in Figure 4 but on a logarithmic scale, and the modeled distribution using eq. 1 and eq.2 (red line).

From Figure 5 it becomes clear that this analysis will require a large number of simulations, since for every wave with maximum amplitude of meter per second we need thousands of waves with maximum amplitudes of decimeters per second. To simplify the procedure we assume that the cirrus clouds formed in waves always behave the same.

In Figure 6 the blue line represents the evolution of relative humidity in a case when no clouds are formed (RHpot). The pink line represents the evolution for a hypothetical cloud. At some point crystals appear (RHform). Shortly thereafter the maximum relative humidity is reached (RHmax). The humidity relaxes to saturation levels (RHsat). The humidity remains at saturation levels even in the downdraft for some time before the evaporating crystals no longer can supply the ambient air with enough water vapor to retain near saturation levels (RHevap).

We make use of the formulations already introduced and describe the variation in the humidity by,

$$RHi(t) = 55\left(amp\sin(\pi \frac{t}{T}) + \frac{amp}{2}\sin(\pi \frac{t}{T}) \right) + 100 \quad (3)$$

And the cloud water content by

$$CWC(t) = C\left(amp\cos(\pi \frac{t}{T}) + amp \right) \quad (4)$$

These two parameters are presented in Figure7.

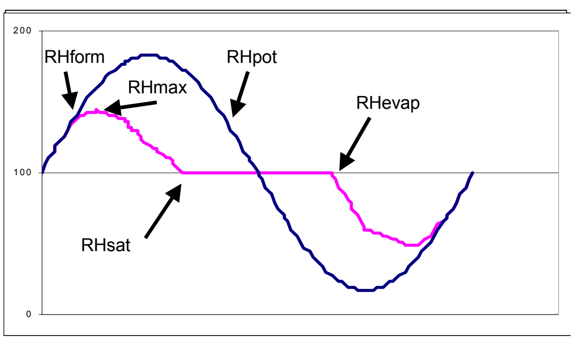

Figure 6. The temporal evolution of relative humidity for the case without cloud formation and for a hypothetical case. See text for notations.

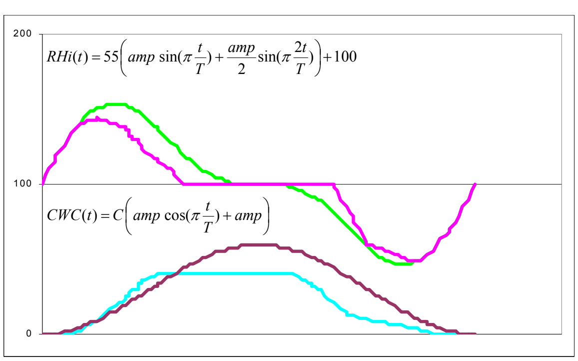

Figure 7. The prescribed temporal evolution of relative humidity (green line) and cloud water content (purple line) in the modeled cirrus cloud. Pink and blue line represents a hypothetical cloud.

Moreover we assume that the number of crystals formed in the cloud is determined by the peak relative humidity reached. The relation used in this work was essentially picked from the data and is shown in Figure 8. Although, for the final result this is not critical as long as the number of crystals formed increase strongly with increasing relative humidity.

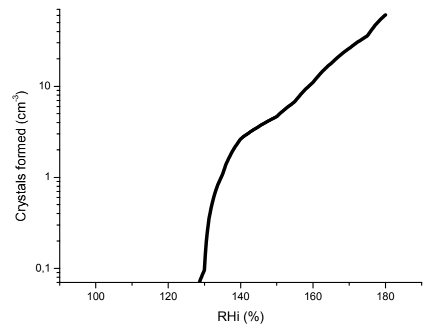

Figure 8. The relation between relative humidity and the number density of crystals formed.

The formulation for evaporation presented in eq. 5 is given by two terms. One is related to the humidity and the other to the crystal number density.

$$Nc = Nc_{n-1} = \left(1 - \left(\frac{100 - RHi}{100}\right)\right)\left(1 - \left(\frac{Nc_{n-1}}{40}\right)^{0.8}\right) \quad (5)$$

The idea is that with a larger number of crystals the rate at which the crystals disappear is larger. Finally, the size of the crystals is simply proportional to the cloud water content divided by the crystal number density.

$$Size = \left(C\frac{CWC}{Nc} \right)^{\frac{1}{3}} \quad (6)$$

As seen from the formulations above this is not an attempt to simulate cirrus, but rather to mimic the behavior of cirrus clouds. We now have a set of extremely simple relations, which allows making thousands of simulations in a very short time period.

As expected, the calculations of average vertical wind, presented in Figure 9, show similar features as the observations. The vertical wind in Figure 9 show the updraft/downdraft regions around the 100% RHi as well as the gradient along a given crystal number density.

The calculated equivalent of Figure 1 is presented in Figure 10. In this figure no distinction is made about crystal size and all particles formed as crystals are counted. The data in Figure 1 is based on the measurements by the CVI. The probe used in the INCA experiment has a lower cut-off of approximately 5 μm aerodynamic diameter, which means that crystals smaller than this size are not sampled. We emulate the probe selection of crystals by setting a size threshold on the calculated results.

Figure 11 show that the areas removed by the size selection is the highest number densities and the highest humidities. Figure 11 and figure 1 are of course not identical but this simple approach gives some in sight to why a maximum is found in figure 1. Note also that the emulated cirrus cloud represents one initial ambient condition only and mixing or precipitation is not included.

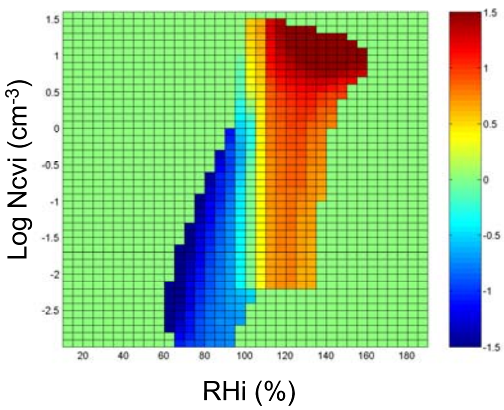

Figure 9. Average calculated wind (c.f. Figure 3).

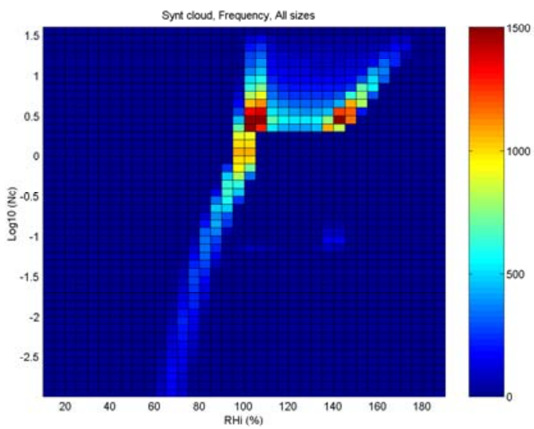

Figure 10. Calculated frequency of occurrence as a function of relative humidity and crystal number density.

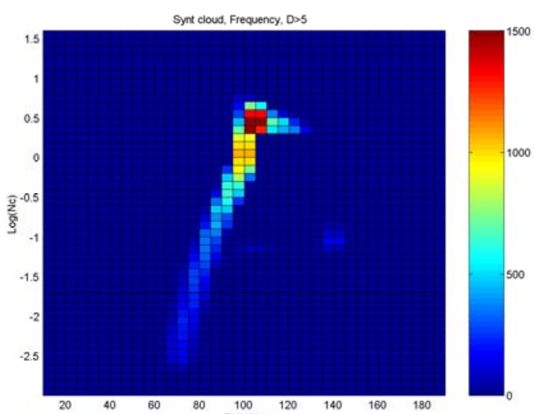

Figure 11. Same as Figure 10, but small particles are not counted in the frequency distribution.

The normalized version of Figure 11 is presented in Figure 12. In this case the formation threshold was set to 140% RHi. In Figure 13 the formation threshold was sat at a humidity 10% lower. The difference between the two figures is that at a lower humidity threshold the U-shapes pattern found in Figure 2 appears.

The probability to observe a particular combination of crystal number density and relative humidity is given by how often a humidity is reached and how long time the cloud remain at the at humidity. The highest humidities are reached only occasionally, but all clouds will converge at 100% RHi. When a cloud forms, crystals appear quickly and the cloud stay for a very short time at high humidities and low crystal number densities. At humidities below 100%, the probability to find a cloud of course decrease with decreasing humidity.

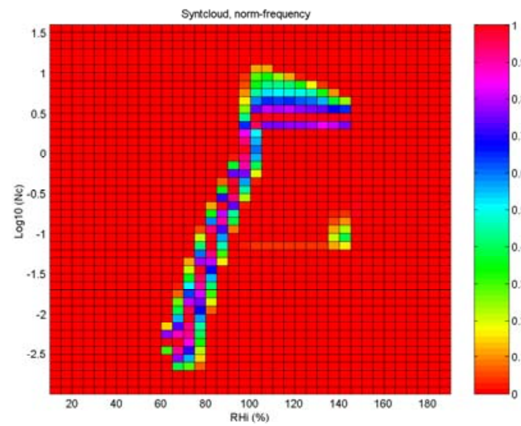

Figure 12. Normalized version of data in Figure 11

Hence, some clouds barely reach the threshold conditions for ice nucleation and then relax towards 100% RHI, whereas some clouds reach much higher humidities than required for cloud formation. Because these different clouds pass through the same combinations of Ncvi and RHI when the clouds form, this cumulative characteristic gives rise to the U-shape in Figure 13.

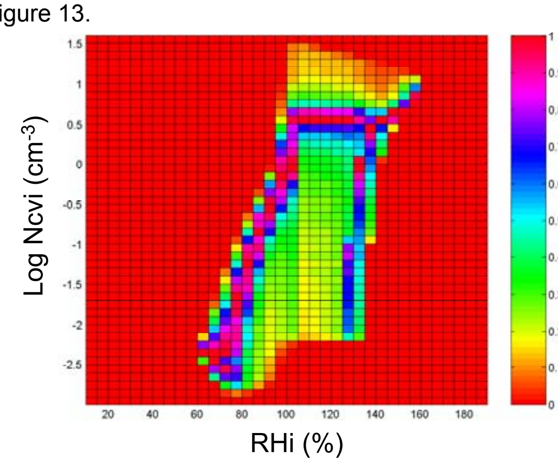

Figure13. As Figure 12, but ice crystals are allowed to form at a lower relative humidity.

The data used in the figures above was from the Pretwick campaign, but the Punta Arenas campaign look very similar.